*Acta Geologica Sinica* (English Edition), 2019, 93(1): 248–249

**Research Advances**

# High Temperature, High Reducibility and Low Productivity of the Paleoceanographic Environment in the P/T, Tethys

JI Changjun[1, 2, *], WU Zhenhan[3], FANG Chaogang[4], YI Haisheng[5] and XIA Guoqing[5]

[1] *Institute of Geomechanics, Chinese Academy of Geological Sciences, Beijing 100037, China*
[2] *Key Laboratory of Paleomagnetism and Tectonic Reconstruction of Ministry of Natural Resources, Beijing 100037, China*
[3] *Chinese Academy of Geological Sciences, Beijing 100037, China*
[4] *Nanjing Center, China Geological Survey, Nanjing 210016, China*
[5] *Institute of Sedimentary Geology, Chengdu University of Technology, Chengdu 610059, China*

Citation: Ji et al., 2019. High Temperature, High Reducibility and Low Productivity of the Paleoceanographic Environment in the P/T, Tethys. *Acta Geologica Sinica* (English Edition), 93(1): 248–249. DOI: 10.1111/1755-6724.13658

## Objective

In the Permian–Triassic geological history, the Tibet Tethys domain deposited continuous marine carbonate strata and recorded information related to the largest bioextinct events in the life history of the earth (Ji Changjun, 2018). The complete Permian–Triassic conodont sequence has been established in the northern margin of the Coqin Basin (Zhou Liqian, 2012), which provides a time scale for the study of the paleoceanographic environment evolution in the Tibet Tethys field at the turn of the P/T. This work selected the total organic carbon and sulfur content of the rocks, carbon and oxygen isotopes of carbonate rocks, and the organic carbon isotope index system to study the evolution of the paleo marine environment in this period.

## Methods

At the Permian–Triassic boundary of the Wenbudangsang section, the samples were collected at the same distance of 5 cm, so as to avoid sampling of later rock alteration, calcite vein filling, pyrite crystal filling, joint and breakage, and to optimize the fresh muddy limestone. These samples were examined under a microscope and cathodoluminescence analysis was conducted. Most samples have a typical microcrystalline structure, and have weak cathodoluminescence characteristics, showing low Fe and Mg content, which can reflect the ancient ocean information. The content of total organic carbon and sulfur is determined by a carbon and sulfur analyzer with an analytical accuracy of 0.1%. The carbon and oxygen isotopes of carbonate rocks were determined by the phosphoric acid method. The isotopes of organic carbon were determined by the high temperature burning method. The isotopes are relative to the PDB standard and the analytical accuracy is 0.20 per thousand. Sample analysis was completed at the analytical and testing center of Beijing Research Institute of Uranium Geology, CNNC.

* Corresponding author. E-mail: jichangjun2007@sina.com

## Results

In this study, the test data of 38 samples were obtained, and the change trend of the paleoceanographic environment index in Tibet Tethys domain was recorded at the turn of P/T (Fig. 1). (a) The ratio of C/S increased rapidly and then tended to be stable, indicating that the reducing PTB of the sea water reached the maximum and

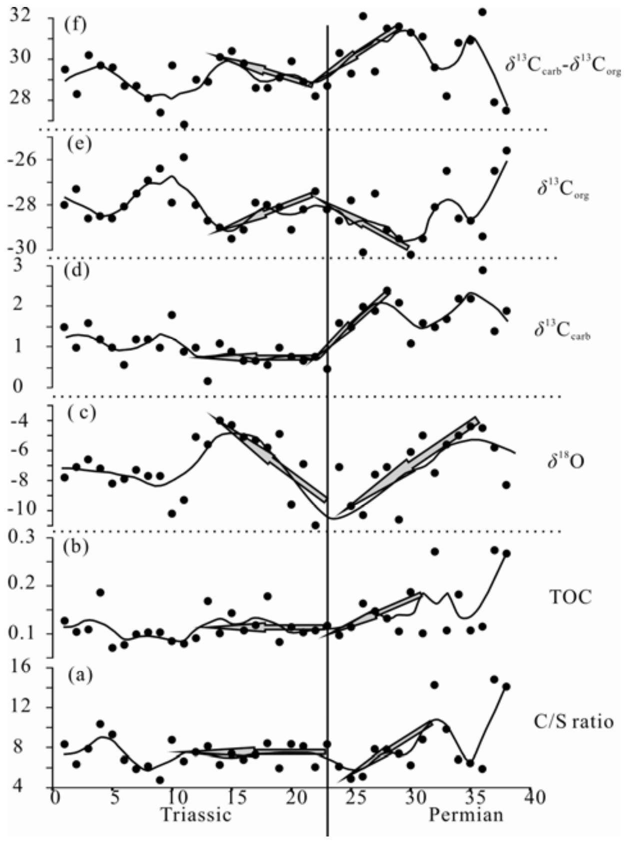


Fig. 1. The evolution of paleoceanographic environment in the Tibet Tethys region at the ture of Permian–Triassic geological history.


http://www.geojournals.cn/dzxbcn/ch/index.aspx
https://onlinelibrary.wiley.com/journal/17556724

then tended to be stable; (b) TOC content decreased and then increased, indicating that the ancient marine productivity of PTB reached the lowest level and decreased with the biological extinction; (c) During the Permian–Triassic period, there is a trough of $\delta^{18}$O curve indicating that the ocean is in a warm period, and the temperature of water reached its maximumin in end-Permian; (d), $\delta^{13}C_{carb}$ gradually decreased and then tended to be steady; (e) $\delta^{13}C_{org}$ gradually increased, and then decreased; (f) $\Delta\delta^{13}C=\delta^{13}C_{carb}-\delta^{13}C_{org}$ gradually decreased and then increased.

## Conclusions

In the Permian–Triassic period, the carbonate strata have recorded the evolution of paleoceanographic environment in Tethys, Tibet. There are negative inorganic carbon anomalies and positive organic carbon anomalies, and there is a significant negative correlation between $\delta^{13}C_{carb}$ and $\delta^{13}C_{carb}$. $\delta^{13}C_{carb}-\delta^{13}C_{org}$ and $\delta^{13}C_{carb}$ are positively correlated in these period. This means that during this period, the dominant mechanism for controlling carbon cycle did not change greatly. The anomalous change is only transient and near PBT, which is caused by the buffering effect of the huge DOC Library in the deep sea. The variation of $\delta^{13}C_{carb}$ and $\delta^{13}C_{carb}$ near PBT is closely related to the evolution of the paleoceanographic environment (Yin et al, 2001; Ji Changjun, 2018). The paleoceanographic environment has undergone dramatic changes during the Permian–Triassic period, when its main performance the reducing of the sea water reached the maximum, and the temperature of water reached the maximum and productivity of ocean reached the minimum in end-Permian.

## Acknowledgments

This research was financially supported by the National Natural Science Foundation of China (grant No. 41602122), the National Technological Projects (grant No. 2016ZX05034-001-003) and the China Geological Survey (grant No. DD20160161).

## References

Ji Changjun, Wu Zhenhan Yi Haisheng, Xia Guoqing, Zhao Zhen and Wang Ting, 2018. The significance of $^{13}$C-$^{18}$O isotopic excursion of the carbonates rock at the PTB in the Wenbudangsang section, Tibet. *Acta Geologica Sinica*, 92 (10): 2018–2027.

Zhou Liqian, 2012. In-situ SHRIMP oxygen isotopic study on conodonts from the Permian/Triassic boundary of Wenbudangsang section, Tibet. *Chengdu University of Technology* (master thesis), 1–70 (in Chinese with English abstract).

Yin, H.F., Zhang K.X., Tong J.N., Yang Z.Y., and Wu S.B., 2001.The global stratotype section and point (GSSP) of the Permian–Triassic boundary. *Episodes*, 24(2): 102–114.

**Appendix 1 Evolution of paleoceanographic environment parameters in the Tibet Tethys region at the turn of Permian-Triassic geological history**

| Number | Sample | Period | C/S ratio | TOC | $\delta^{13}C_{org}$ | $\delta^{13}C_{carb}$ | $\delta^{18}O$ | $\Delta\delta^{13}C$ |
|---|---|---|---|---|---|---|---|---|
| 1 | WB1 | | 8.30 | 0.13 | −28 | 1.5 | −7.8 | 29.5 |
| 2 | WB 2 | | 6.34 | 0.10 | −27.3 | 1 | −7.1 | 28.3 |
| 3 | WB 3 | | 7.84 | 0.11 | −28.6 | 1.6 | −6.6 | 30.2 |
| 4 | WB 4 | | 10.33 | 0.19 | −28.5 | 1.2 | −7.2 | 29.7 |
| 5 | WB 5 | | 9.28 | 0.07 | −28.6 | 1 | −8.2 | 29.6 |
| 6 | WB 6 | | 6.76 | 0.08 | −28.1 | 0.6 | −7.9 | 28.7 |
| 7 | WB 7 | | 5.86 | 0.10 | −27.5 | 1.2 | −7.3 | 28.7 |
| 8 | WB 8 | | 6.13 | 0.10 | −26.9 | 1.2 | −7.7 | 28.1 |
| 9 | WB 9 | | 4.75 | 0.10 | −26.4 | 1 | −7.7 | 27.4 |
| 10 | WB 10 | | 8.74 | 0.08 | −27.9 | 1.8 | −10.2 | 29.7 |
| 11 | WB 11 | | 6.63 | 0.08 | −25.9 | 0.9 | −9.3 | 26.8 |
| 12 | WB 12 | Triassic | 7.52 | 0.09 | −28 | 1 | −5.1 | 29 |
| 13 | WB 13 | | 8.12 | 0.17 | −28.7 | 0.2 | −5.6 | 28.9 |
| 14 | WB 14 | | 6.27 | 0.10 | −29 | 1.1 | −4 | 30.1 |
| 15 | WB 15 | | 7.37 | 0.14 | −29.5 | 0.9 | −4.3 | 30.4 |
| 16 | WB 16 | | 6.77 | 0.11 | −29.1 | 0.7 | −5.1 | 29.8 |
| 17 | WB 17 | | 7.28 | 0.12 | −27.9 | 0.7 | −5.3 | 28.6 |
| 18 | WB 18 | | 8.40 | 0.18 | −28 | 0.6 | −5.8 | 28.6 |
| 19 | WB 19 | | 5.93 | 0.08 | −28.1 | 1 | −4.9 | 29.1 |
| 20 | WB 20 | | 8.32 | 0.11 | −29.1 | 0.8 | −9.6 | 29.9 |
| 21 | WB 21 | | 8.11 | 0.10 | −28.2 | 0.7 | −6.9 | 28.9 |
| 22 | WB 22 | | 6.05 | 0.11 | −27.4 | 0.8 | −10.9 | 28.2 |
| 23 | WB 23 | | 8.30 | 0.12 | −28.2 | 0.5 | −3.5 | 28.7 |
| 24 | WB 24 | | 6.10 | 0.10 | −28.7 | 1.6 | −7.1 | 30.3 |
| 25 | WB 25 | | 4.87 | 0.11 | −27.8 | 1.5 | −9.7 | 29.3 |
| 26 | WB 26 | | 5.11 | 0.16 | −30.1 | 2 | −10.3 | 32.1 |
| 27 | WB 27 | | 7.82 | 0.15 | −27.5 | 1.9 | −7.6 | 29.4 |
| 28 | WB 28 | | 7.76 | 0.13 | −29.1 | 2.4 | −7.1 | 31.5 |
| 29 | WB29 | | 7.39 | 0.11 | −29.5 | 2.1 | −10.6 | 31.6 |
| 30 | WB 30 | Permian | 6.23 | 0.19 | −30.2 | 1.1 | −6.1 | 31.3 |
| 31 | WB31 | | 8.78 | 0.10 | −29.5 | 1.6 | −5 | 31.1 |
| 32 | WB 32 | | 14.26 | 0.27 | −28.1 | 1.5 | −7.5 | 29.6 |
| 33 | WB 33 | | 9.82 | 0.11 | −26.5 | 1.7 | −5.6 | 28.2 |
| 34 | WB34 | | 6.79 | 0.18 | −28.6 | 2.2 | −5 | 30.8 |
| 35 | WB 35 | | 6.45 | 0.11 | −28.7 | 2.2 | −4.4 | 30.9 |
| 36 | WB 36 | | 5.87 | 0.12 | −29.4 | 2.9 | −4.5 | 32.3 |
| 37 | WB 37 | | 14.81 | 0.27 | −26.5 | 1.4 | −5.8 | 27.9 |
| 38 | WB 38 | | 14.05 | 0.27 | −25.6 | 1.9 | −8.3 | 27.5 |